Hardware factors influencing interlayer bonding strength of parts obtained by Fused Filament Fabrication

Vladimir E. Kuznetsov*, Azamat G. Tavitov, Oleg D. Urzhumtsev

Department of Physical Metallurgy of Non-Ferrous Metals, National University of Science and Technology "MISIS", Leninskiy Prospekt 4, NUST MISIS, 119049 Moscow, Russia; aztapps@gmail.com (A.G.T.); darikcr@gmail.com (O.D.U.)
* Correspondence: kuznetsovve@misis.ru; Tel.: +7-926-231-2760

Abstract

Current paper investigates the influence of hardware setup and parameters of a 3D printing process based on fused filament fabrication (FFF) technology on resulting sample strength.
Three-point bending of samples printed with long side oriented along Z axis was used as a measure of the interlayer bonding strength. The same CAD model was converted into NC-programs through same slicing software to be run on four different desktop FFF 3D printers, out of filament of same brand and color. Within all the printers same ranges of layer thickness values from 0.1 to 0.3 mm and feed rates from 25 to 75 mm/s were planned to be varied.
All the machines demonstrated statistically almost identical values of maximum flexural strength, however the different machines exhibited maximum sample strength with different combinations of varied parameters. Among all the hardware factors observed, the most important was proved to be extruder type, direct or Bowden. This feature fundamentally changes the nature of studied parameters influence onto the resulting strength of the FFF process. For the extruders of Bowden type the length of flexible guiding tube is of great importance.

Keywords: Fused Filament Fabrication; Fused Deposition Modeling; interlayer bonding; direct extruder; Bowden extruder

In the current work, the following notions are introduced and the following shorthands are used:

FFF —Fused Filament Fabrication is a technology of digital additive manufacturing based on extrusion and layered deposition of melted thermoplastic. From technological point of view *FFF* is same as *FDM*® — Fused Deposition Modeling, the only difference is that while the *FDM*® is a registered trademark and thus applies to Stratasys machines only, the *FFF* is a term coined inside the RepRap community;
UFL — Ultimate Fracture Load, maximum load observed during mechanical testing;
UFS — Ultimate Fracture Strength, calculated stress in the sample caused by *UFL*;
Sublayer — a layer of plastic already deposited by *FFF* 3D printer which acts as a substrate for layer being deposited at given moment;
Filament — plastic in the filament form used as supply in *FFF* process;
Thread — extruded and deposited thread of plastic mimicking the 3D printed part;
Feed rate — the linear printing speed, the speed of nozzle traveling across XY plane while extruding and depositing the plastic threads;

Flow rate — the volume of plastic delivered through the nozzle per unit time;
Extrusion efficiency — a ratio of real to calculated mass of 3D printed object;
Underextrusion — a characteristic defect in *FFF* process resulting in significant drop in thread thickness or in thread interruptions caused by shortage of *Flow rate* and low extrusion efficiency.

1 Introduction

Among other additive manufacturing technologies used, (polymer) material extrusion remains the most widespread in terms of printed volume (46%) and units sold (75%) [1]. Such a great share of the market is formed mostly by desktop machines, according to [2,3], only in two last years the number of desktop 3D printers in use based on polymer extrusion raised by a million of machines. The popularity of these machines raised due to its simplicity and low cost: a part is built by adding threads of molten polymer, extruded through a hot nozzle. Strength of the parts, obtained by this method, depends largely on bonding between the threads in contact forming same or adjunct layers. The quality of bonding depends in turn on material properties and various parameters of the material extrusion and deposition process.

Before the rise of the RepRap [4,5,6,7] project the only company making machines based on the principle of material extrusion was the Stratasys founded by Scott Crump, the inventor of this approach [8,9,10], which is marketed under FDM® (Fused Deposition Modeling) trademark. The Stratasys printers and accompanying CAM systems (slicers) did not allow the users to vary geometrical and technological parameters beyond predefined limits. For example, Stratasys Dimension Elite allows to choose layer thickness value out of two options — 0.176 mm (0.15") and 0.254 mm (0.2"). Infill density also has two options (high and low), while the shell thickness or any other part geometry parameters, extrusion or environment temperature and printing speed are not configurable at all. Thus, early research [11-21] on 3D printing with molten polymer parts strength are limited by varying the parameters predefined in Stratasys software. After Open Source printers and slicers were developed, users got full control over the process options. Modern slicers allow to set any values (including those beyond physical capabilities of a particular 3D printer) to any parameters, including but not limited to layer thickness, hotend and bed temperatures, linear motion speed, acceleration, cooling fan speed. There are many recent studies on different parameters influencing printed parts strength, including extrusion temperature [21–25], layer thickness [26–31], printing speed [25, 29, 32], part orientation [27,29,31, 33, 34] and constitution [27, 35, 39, 40]. However, the findings often do not fit together, or even can come to direct contradiction. For example, one of key parameters of the FFF is the thickness of layers mimicking the part, which defines the printed part resolution. The work [29] claims that for all variants of printing part orientation, its strength increases with increment of layer thickness, while [30] shows directly opposite results.

One of the key reasons for that discrepancy is the absence of a common methodology to assess FFF printed parts strength. Most of the researches are based on methods described in existing standards [41, 42] for testing monolithic polymer parts which were not designed to handle parts with anisotropic features [43]. Various papers use different printing setups: the samples of standardized shape and dimensions are oriented differently on the bed and are printed with varying constitution (the subset of all possible parameters describing shell, infill and horizontal surfaces) and other parameters (nozzle diameter, temperature). Another feature of these researches is the broad variety of

equipment (namely, 3D printers) used to manufacture the samples for tests. The authors often try to generalize their findings over the whole FFF technology, which might be premature.
Current study aims to:

- check if different machines (3D printers) might exhibit different dependency of the process parameters on sample strength;
- map out the influence of technological and hardware factors on FFF samples strength and to sketch up the future research design.

2 Machines, materials and methods

2.1 Sample shape and dimensions

Recent studies [25, 30] have introduced and verified a relatively simple and informative technique for evaluating the interlayer bonding strength of a part obtained with FFF. The technique is based on three-point bending procedure with loading a sample printed with a long-side oriented along the Z axis (Figure 1). Such an orientation leads to the fact that the maximum stresses in the critical section are acting orthogonally to the layer boundaries, that is, in the direction in which the sample should exhibit the least strength.
Current set of experiments featured tube-shaped samples of rectangular cross-section with 10×20 mm in size, of 120 mm in length with fillets (R = 2 mm) along long ribs (Figure 1). The tube shape of the sample was provided by setting the “infill” parameter to “0” in the slicer interface program (Cura 15.04) [44] and turning off the “solid infill top” and “solid infill bottom” checkboxes. The thickness of the tube wall was defined by the “shell thickness” parameter and was set to 2.4 mm. The choice of this exact shape and sample size was determined by the desire to obtain data compatible with previous studies [25, 30].

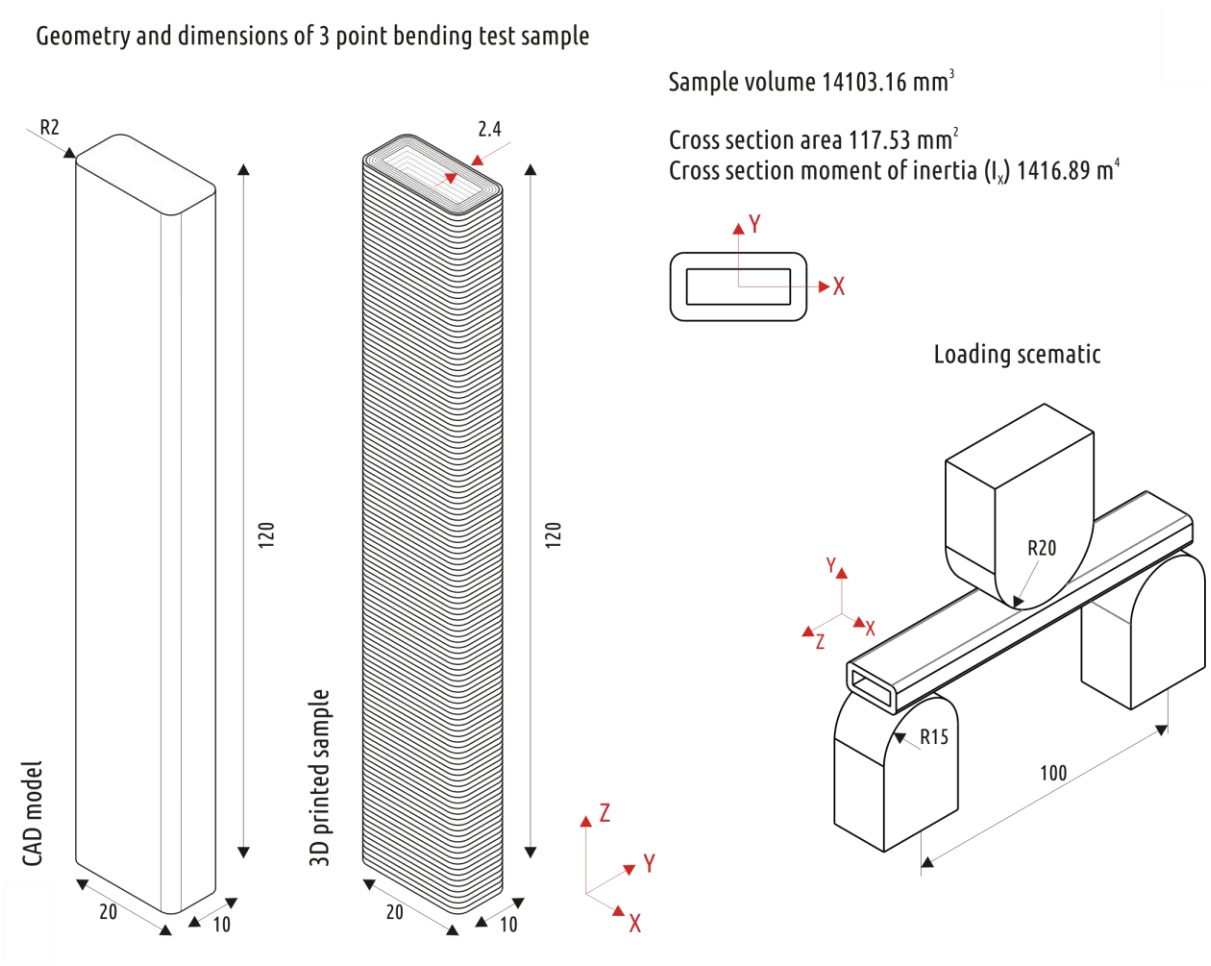

Figure 1. CAD model and 3D printed sample for three point bending

2.2 Samples fabrication

2.2.1 Hardware setups

Four different desktop 3D printers were used in the study: Ultimaker 2 (Ultimaker B.V., Geldermalsen, The Netherlands), 3DQ mini (3DQuality JSC, Moscow, Russia), Original Prusa i3 MK3S (Prusa Research s.r.o., Prague, Czech Republic) and Delta WASP 2040 (WASP c/o CSP S.r.l., Massa Lombarda (RA), Italy). The following short names will be used further for convenience: UM2, 3DQ, PRUSA and WASP for each of the four printers accordingly. All four machines used are based on the FFF technology, but there are significant differences in design. The overview is given in Table 1.

Preprints (www.preprints.org) | NOT PEER-REVIEWED | Posted: 9 May 2019 doi:10.20944/preprints201905.0108.v1

Peer-reviewed version available at Polymers 2019; doi:10.3390/polym11111870

Table 1. Main parameters of 3D printers in the study

Machine	UM2	3DQ	PRUSA	WASP
Scheme	Cartesian	Delta	Cartesian	Delta
Filament diameter, mm	2.85	1.75	1.75	1.75
Extruder type	Bowden	Bowden	Direct	Bowden
Distance from the feeder to the nozzle, mm	700 mm	750 mm	90 mm	200 mm
Movement of part being printed	Along Z	No	Along Y	No
Power of the heater in the melting block, W	35	40	40	2*40
Enclosure	Front and top open	Fully open	Fully open	Closed
Bed surface	Glass	Coated steel+blue scotch tape	Coated steel	Aluminum alloy+blue scotch tape
Heated bed	Yes	Yes	Yes	Yes
Part cooling	2x30 mm fans (12V 0.1A)	2x 40mm centrifugal fan (12V 0.13A)	1x50mm centrifugal fan (5V 0.25A)	1x40mm axial (12V 0.8A)
Acceleration settings used	3000 mm/s² (XYZ)	500 mm/s² (XYZ)	3000 mm/s² (XYZ)	3100 mm/s² (XYZ)
Control board/firmware	8 bit ATMega2560 (Marlin-based)	32 bit Smoothieboard compatible	8 bit ATMega2560 (Marlin-based)	8 bit ATMega2560 (Marlin-based)

2.2.2 Process parameters

The values of the following 3D printing parameters remained constant during all experiments, on all the machines:

- nozzle diameter (0.4 mm);
- heated bed temperature (60 °C);
- extrusion temperature (210 °C);
- the first layer thickness (0.3 mm);
- the first layer printing speed (25 mm/s).

Following parameters were varied:

- machine (UM2, 3DQ, PRUSA and WASP);
- printing
- speed (25, 50 and 75 mm/s);
- layer thickness (0.1 to 0.3 mm with increment of 0.05 mm).

It is worth mentioning that the sample design (shape and dimensions) was originally verified for use with UM2 3D printer. No issues with samples stability while printing with UM2 were observed neither in current nor in earlier studies [25, 30]. However, all other machines in the study incurred

Preprints (www.preprints.org) | NOT PEER-REVIEWED | Posted: 9 May 2019 doi:10.20944/preprints201905.0108.v1

Peer-reviewed version available at Polymers 2019; doi:10.3390/polym11111870

problems with printing part stability. A quick solution was adding brim (20 lines) to the samples printed with 3DQ, PRUSA and WASP.

2.3 Material

A turquoise PLA filament of 1.75 and 2.85 mm gauges was used, produced by REC company (REC, Moscow, Russia). This specific manufacturer of filament was chosen due to locally produced material. All the spools of 1.75 mm came from the same batch produced in February 2019, according to the labels. All the spools of 2.85 mm filament also came from a single batch, produced, however, in June 2018. All the spools were sealed in plastic bags with silica gel and packed into cardboard boxes.
In order to obtain real diameters of the filament utilized both 1.75 and 2.85 mm filaments were measured with digital micrometer. For each of the gauges 81 diameter measurements were performed in nine points on three spools, measured in three different axes with angle of 120° between them. The average diameter for 2.85 mm gauge was 2.833 with standard deviation of 0.017. The average diameter for 1.75 mm gauge was 1.729 with standard deviation of 0.016.

2.4 Sample mass measurement

All samples were weighed before mechanical testing using digital analytical scales ViBRA LF Series (Shinko Denshi Co. LTD, Tokyo, Japan). For samples printed with brim, the brim was torn out before the weighting. Measurement results were rounded to two decimal digits. The extrusion efficiency — calculated to measured mass ratio — is computed on that basis. The calculated mass (17.47 g) can be determined by the estimated sample volume (14.10 cm^3) multiplied by PLA density (1.24 g/cm^3).

2.5 Mechanical testing

The samples were tested with a universal 50 kN electromechanical testing machine IR 5057-50 (OOO Tochpribor, Ivanovo, Russia) with a test rig for three-point bending. The samples rested on two cylindrical supports of 30 mm diameter with a distance of 100 mm between the centers, the load was put on the middle of the sample between the supports by a cylinder of 40 mm in diameter.
The tests were carried out with the crosshead of the tensile tester moving at a speed of 10 mm/min. During the test, the displacement and load were recorded, the initial load for sample stabilization being set at 5N. The key parameter registered was the maximum load measured before the samples failed (UFL).
For a more general discussion of results obtained, the normal stresses in the samples at the moment of failure (UFS) were calculated. The stresses were calculated by dividing the maximum moment (M) by the section modulus (W):
$UFS = \frac{M}{W}$, MPa.
The maximum moment for testing samples at distance between the supports (l) of 100mm
$M = \frac{F \times l}{4} = 0.025F$, N·m,
where F is the load in N at the moment of failure (UFL).
The section moment is calculated by using formula:

$W = \frac{2I}{h}, m^3,$

Preprints (www.preprints.org) | NOT PEER-REVIEWED | Posted: 9 May 2019 doi:10.20944/preprints201905.0108.v1

Peer-reviewed version available at Polymers 2019; doi:10.3390/polym11111870

where I is the second moment of the cross-section, calculated with the built-in app of SolidWorks to be 1416.89 mm^4.
Thus, the maximum normal stress in the sample can be calculated from the load by
$UFS=0.088F$,
where F is given in N and UFS is in MPa. Since the only method of measuring mechanical performance of FFF samples was applied, for the sake of simplicity, term "Strength" will be used instead of Ultimate Flexural Strength.

2.6 Printing sample temperature evaluation

Temperature distribution over the surface of some samples was recorded during printing process using a FLIR B335 (FLIR Systems, Wilsonville, OR, USA) thermal imager with a resolution of 320×240 pixels. The camera was located in front of the printer. Thermal imaging was carried out at the height of the sample being printed between 55 and 65 mm (approximately in the area in which further destruction at the three-point bend occurred). The survey was carried out from a distance of about 30 cm, which is equal to minimal focal distance documented for the imager.
The software "FLIR Tools" [45] was used to determine the average temperature on the surface of the sample at a distance of 1 to 3 mm from the lower cut of the nozzle (Figure 2). This temperature was taken as the sublayer temperature.

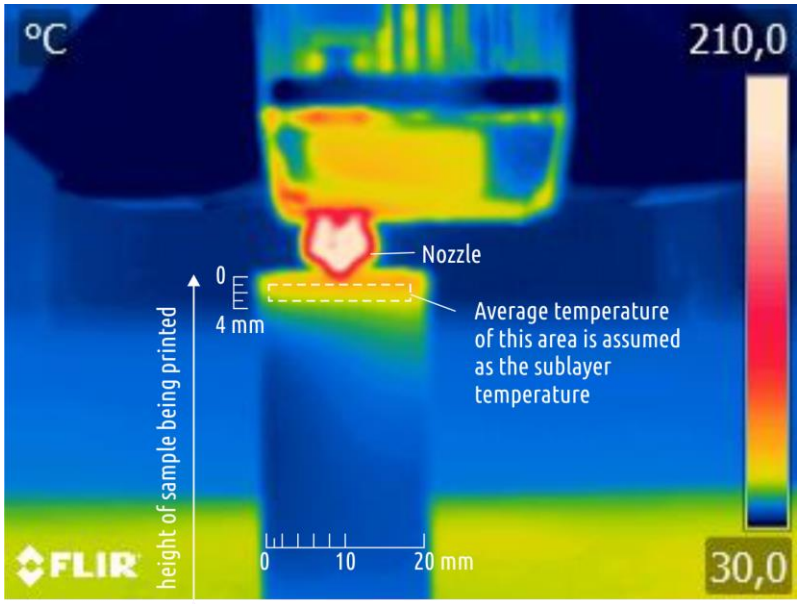

Figure 2. Typical IR image and the area for averaging the temperature with FLIR Tools for taking as the sublayer temperature

3 Results

The complete experiments plan was only fulfilled on the WASP machine and with certain limitations on PRUSA. The samples printed on PRUSA with 0.3 mm layers at 75 mm/s linear motion speed have distinctive defects caused by sample oscillation. The defective zone does not lie in destruction area at three-point bending test and thus these samples were not excluded from the scope. Samples printed on UM2 machine with speed of 50 mm/s with layer thickness of 0.25 mm and above, and samples printed with 75mm/s speed and 0.2mm layer and above contained explicit underextrusion defects

Preprints (www.preprints.org) | NOT PEER-REVIEWED | Posted: 9 May 2019 doi:10.20944/preprints201905.0108.v1

Peer-reviewed version available at Polymers 2019; doi:10.3390/polym11111870

and were excluded. 3DQ machine could not provide reliable motion at 75 mm/s, and samples printed at 50 mm/s speed suffered from underextrusion even with 0.2mm layer and thus were excluded. The results obtained are summarized in Tables 2 to 5.

Table 2. Experimental results for the UM2 3D printer

Layer thickness, mm	Feed rate, mm/s	Sample mass, g		Extrusion efficiency	Sublayer temperature, °C	Strength, MPa	
		Mean	SD			Mean	SD
0.1	25	15.95	0.17	0.91	47	49.1	4.7
0.15	25	15.56	0.07	0.89	48	41.91	2.23
0.2	25	15.10	0.07	0.86	50	38.54	1.25
0.25	25	14.34	0.3	0.82	50	20.7	5.86
0.3	25	14.06	0.66	0.8	52	13.43	7.9
0.1	50	15.12	0.09	0.87	49	47.01	3.12
0.15	50	14.27	0.09	0.82	52	39.56	3.93
0.2	50	13.01	0.18	0.74	54	24.61	0.88
0.1	75	14.4	0.13	0.82	50	34.64	1.32
0.15	75	13.85	0.05	0.79	52	21.3	1.87

Table 3. Experiments summary for the 3DQ 3D printer

Layer thickness, mm	Feed rate, mm/s	Sample mass, g		Extrusion efficiency	Sublayer temperature, °C	Strength, MPa	
		Mean	SD			Mean	SD
0.1	25	15.70	0.06	0.90	35	44.73	4.67
0.15	25	15.76	0.13	0.90	35	42.06	1.61
0.2	25	15.27	0.14	0.87	36	28.25	3.07
0.25	25	15.06	0.20	0.86	39	22.57	9.12
0.3	25	14.58	0.13	0.83	40	10.08	1.85
0.1	50	15.25	0.1	0.87	36	19.62	1.31
0.15	50	14.46	0.01	0.83	40	16.84	3.56

Table 4. Experiments summary for PRUSA 3D printer

Layer thickness, mm	Feed rate, mm/s	Sample mass, g		Extrusion efficiency	Sublayer temperature, °C	Strength, MPa	
		Mean	SD			Mean	SD
0.1	25	16.52	0.17	0.95	33	42.17	5.92
0.15	25	16.59	0.16	0.95	33	46.41	4.53
0.2	25	16.66	0.22	0.95	34	49.32	4.32
0.25	25	16.87	0.27	0.97	35	46.16	2.92
0.3	25	16.77	0.16	0.96	36	29.99	5.61
0.1	50	16.38	0.19	0.94	35	40.3	5.29
0.15	50	16.78	0.07	0.96	36	46.23	5.74
0.2	50	16.55	0.15	0.95	36	41.65	7.59
0.25	50	17.00	0.07	0.97	37	36.75	7.6
0.3	50	16.66	0.16	0.95	38	25.55	3.02
0.1	75	16.72	0.23	0.96	36	36.61	7.09
0.15	75	16.78	0.07	0.96	36	34.06	7.9
0.2	75	16.6	0.1	0.95	37	24.05	3.91
0.25	75	17.0	0.07	0.97	38	21.77	1.34
0.3	75	16.66	0.15	0.95	39	19.39	5.52

Preprints (www.preprints.org) | NOT PEER-REVIEWED | Posted: 9 May 2019 doi:10.20944/preprints201905.0108.v1

Peer-reviewed version available at Polymers 2019; doi:10.3390/polym11111870

Table 5. Experiments summary for WASP 3D printer

Layer thickness, mm	Feed rate, mm/s	Sample mass, g		Extrusion efficiency	Sublayer temperature, °C	Strength, MPa	
		Mean	SD			Mean	SD
0.1	25	16.59	0.24	0.95	33	39.67	3.71
0.15	25	16.83	0.18	0.96	33	44.59	1.8
0.2	25	16.54	0.32	0.95	33	35.85	0.48
0.25	25	16.89	0.04	0.97	34	28.03	3.39
0.3	25	16.56	0.18	0.95	34	26.84	3.99
0.1	50	16.68	0.02	0.95	35	34.88	2.19
0.15	50	16.76	0.06	0.96	36	34.99	2.48
0.2	50	16.6	0.17	0.95	37	36.83	1.93
0.25	50	16.53	0.11	0.95	38	23.61	2.25
0.3	50	16.73	0.17	0.96	40	27.81	3.87
0.1	75	16.53	0.19	0.95	36	22.85	2.08
0.15	75	16.54	0.06	0.95	37	31.12	0.82
0.2	75	16.38	0.1	0.94	40	26.96	5.67
0.25	75	16.76	0.08	0.96	42	28.16	2.38
0.3	75	16.48	0.15	0.94	45	16.66	1.6

Sublayer temperature of the samples printed differs significantly depending on machine (see Figure 3). That can be explained by the design differences between machines considered, primarily by the case type and cooling system design and performance.

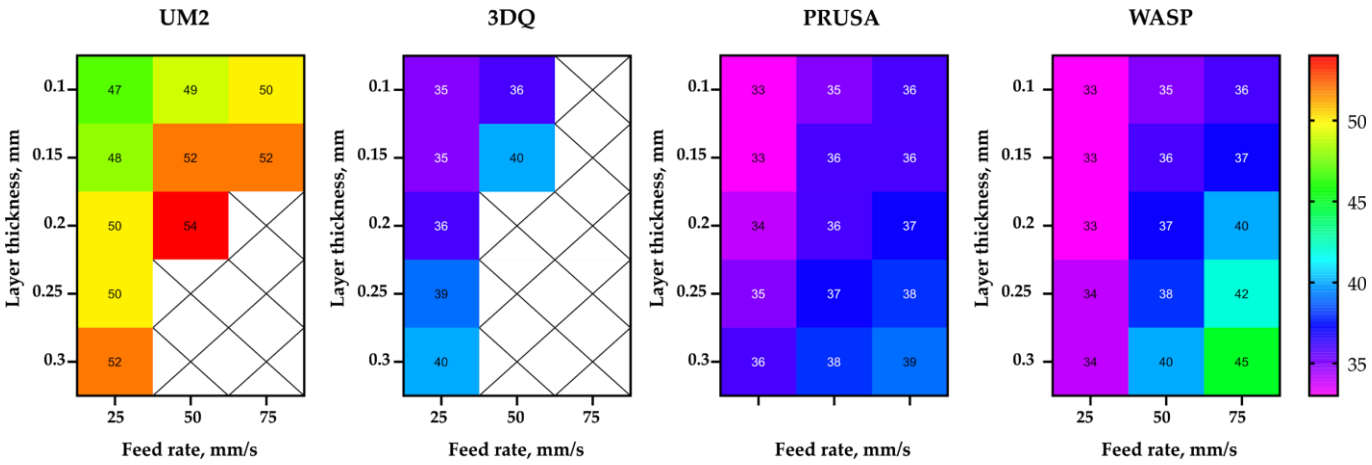

Figure 3. Sublayer temperature depending on feed rate, layer thickness and printer type

The maximum strength values recorded for each machine considered are nearly at the same level of ~47 ±2.5 MPa. However, the dependency of sample mass and strength on layer thickness and printing speed had different nature on machines of different kinds (see Figure 4).

Preprints (www.preprints.org) | NOT PEER-REVIEWED | Posted: 9 May 2019 doi:10.20944/preprints201905.0108.v1

Peer-reviewed version available at Polymers 2019; doi:10.3390/polym11111870

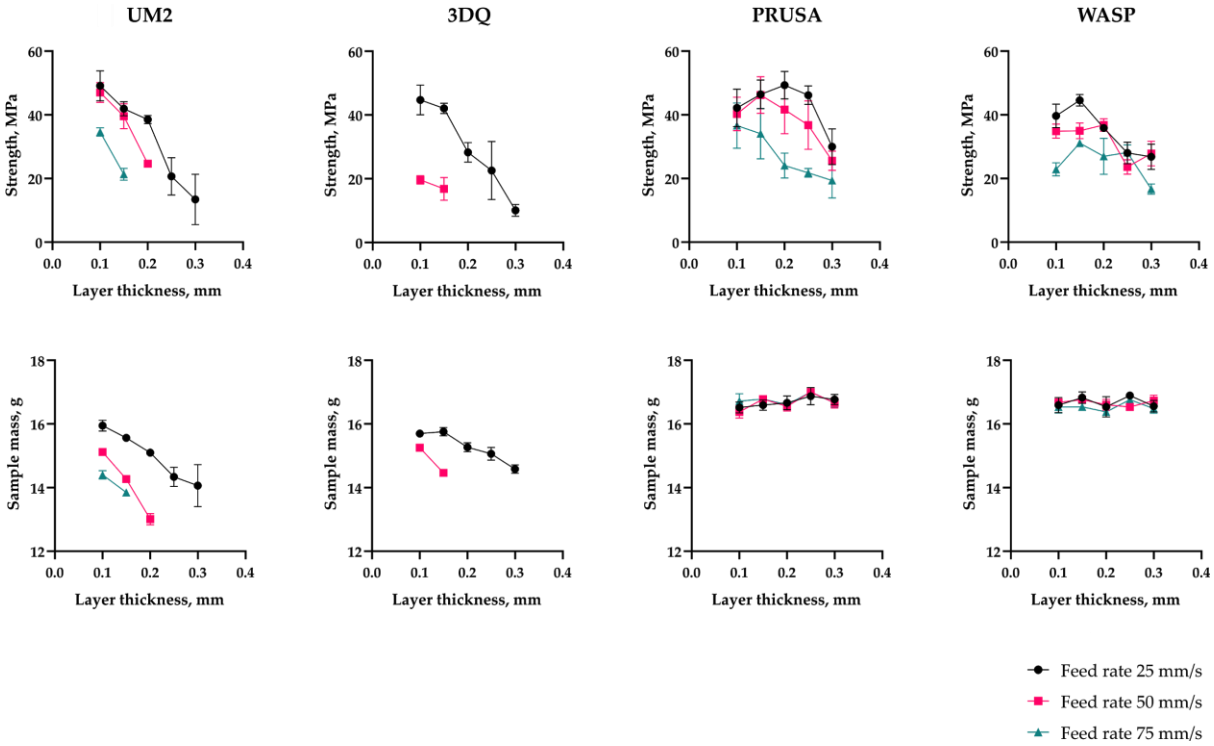

Figure 4. Sample strength and mass depending on layer thickness, feed rate and printer type

4 Discussion

4.1 Bowden vs direct: extruder type influence

In the context of the study type of the extruder (Figure 5) appeared to be the most significant feature of the hardware setup.

Preprints (www.preprints.org) | NOT PEER-REVIEWED | Posted: 9 May 2019 doi:10.20944/preprints201905.0108.v1

Peer-reviewed version available at Polymers 2019; doi:10.3390/polym11111870

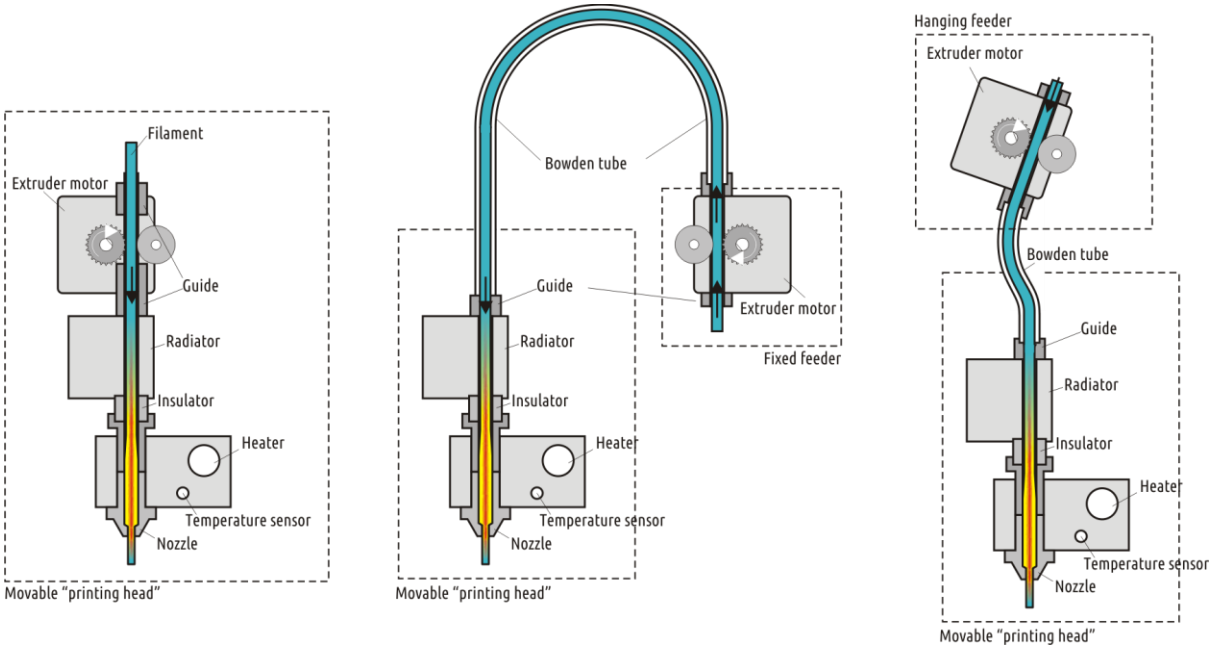

Figure 5. Three types of extruder considered in the study: direct (a), Bowden (b) and Bowden with short tube and hanging feeder (c)

In the extruders of Bowden type the extrusion efficiency strictly depends on the extrusion resistance. Within a single hardware setup with Bowden extruder, extrusion efficiency linearly drops when increasing the flow rate (with increasing layer thickness or feed rate). Eventually, increasing flow rate will result in visible underextrusion defects. On the contrary, extruders of the direct type work literally in binary mode. When the flow rate is within the hardware productivity limit, it does not affect the extrusion efficiency. When the flow rate goes beyond the limit, the extrusion gets interrupted (the extruder motor begins to skip steps or the toothed drive wheel starts to carve filament instead of pushing it forward).

The Bowden extruder with a short tube (WASP) demonstrates behavior similar to the direct extruder (PRUSA) — it does not suffer from the extrusion resistance. In the whole range of the flow rate values tested the mass of samples remains statistically constant. Difference between Bowden and direct or short tube Bowden extruders is well illustrated by plots of sample mass vs flow rate (Figure 6). The extrusion efficiency affects directly the layer bonding area and thus the bonding strength; it is verified by current and previous studies [25, 30].

Preprints (www.preprints.org) | NOT PEER-REVIEWED | Posted: 9 May 2019 doi:10.20944/preprints201905.0108.v1

Peer-reviewed version available at Polymers 2019; doi:10.3390/polym11111870

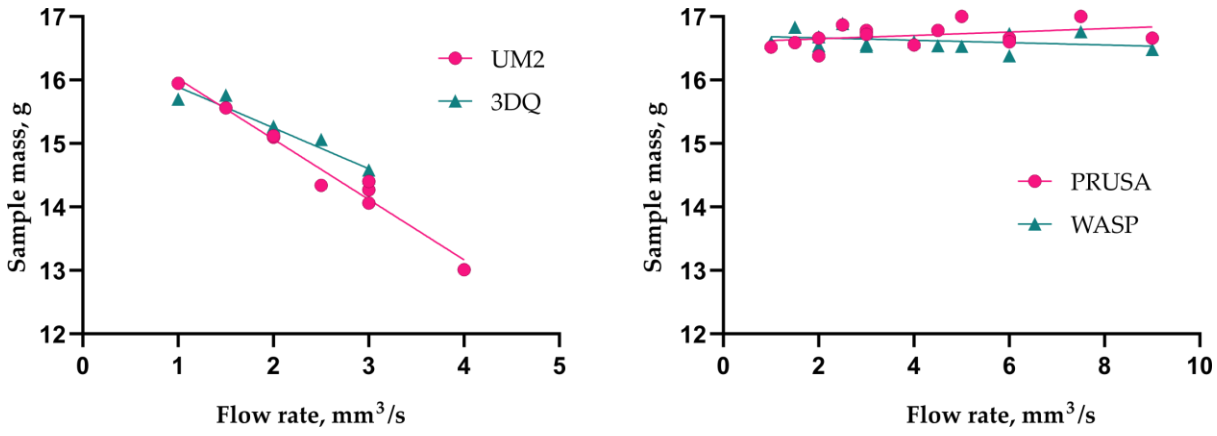

Figure 6. Sample mass dependence on flow rate for printers with Bowden (a) and direct or Bowden with short tube (b) type of extruder

4.2 Cartesian vs delta: influence of motion scheme

Current study did not reveal neither significant advantages not drawbacks of both Cartesian and delta motion systems. Delta printers are more sensitive to increased printhead weight, thus they often feature Bowden extruders, which can be treated as a drawback. However, Bowden extruder with shorter tube used on WASP machine demonstrated results close to PRUSA direct extruder. Considering printing stability and sample surface quality, the following can be said. The coordinate system has smaller influence on print quality than implementation accuracy, especially at higher printing speed (above 40 mm/s). The PRUSA with Cartesian coordinate system uses the bed moving along Y axis, resulting in significant vibrations and oscillations of a sample having high height to bed surface projection ratio. They lead to affluxes and other imperfections on the surface, and even grave defects. The delta-shaped WASP printer also has significant vibrations at 75 mm/s speed, thus careful bed setup was required to ensure prints not to be torn away during printing process. It also seems that high-speed printing on WASP machine is not only limited by the mechanics but by the limited performance of an 8-bit controller that is recalculating linear motion in Cartesian coordinates into gentle movement of all three motors. The 3DQ printer with similar mechanical scheme features more powerful 32-bit controller, however high linear feed rates were spoiled by poor linear guides and carriages with loose coupling. Finally, the Cartesian UM2 contains a bed that is moved along Z axis, while the lightweight printing head has similar motion mechanism along both X and Y axes. There were no stability issues even at high printing speeds. However, high-speed printing (75 mm/s) was limited to layers of 0.1 and 0.15 mm only due to limited extruder performance.

4.3 Thick vs thin: filament diameter influence

There was no significant difference discovered for filaments of two popular gauges. The only machine using 2.85mm filament, the UM2, exhibited results very close to 3DQ. The latter also features Bowden-type extruder but consumes 1.75mm filament. Further research is needed to set up an experiment involving two similar machines with the only difference between them being the consumable filament gauge.

4.4 Open vs closed: printer enclosure and cooling conditions

Even with same temperature values set for the nozzles and heated beds and maximum cooling fan speed, there was some variance in sublayer temperature registered, which has very high influence on layers cohesion strength [25].

Depending on layer thickness and printing speed, the sublayer temperature varied between 48°C to 54°C on UM2 machine, with printing area enclosed from four sides. Printers with open setup featured lower sublayer temperatures: 34 to 39°C on PRUSA and 35 to 40°C on 3DQ machine. That difference could be explained by slightly more efficient cooling subsystem in PRUSA.

It can be stipulated that the partially enclosed UM2 machine has certain advantage over open ones, e.g. PRUSA. So, the maximum strength value obtained on UM2 is almost equal to the maximum value for PRUSA. While PRUSA has significantly better extrusion efficiency, perhaps, the higher sublayer temperature compensates the lack of extruded material.

Finally, the fully enclosed WASP machine exhibited sublayer temperatures in the range of 35 to 45°C, which is more typical for the open type printers. That could be explained by the design and power of the cooling system. Unlike all other machines considered, there is single cooling fan used that pumps the air through hotend radiator onto printed part on two sides of the nozzle. With power consumption of 0.8A at 12V at full speed, it seems that the fan in WASP provides the most intensive airflow of all machines considered.

4.5 Printing speed influence with respect to hardware setup

In general, increasing printing speed resulted in decrease of sample strength for all machines considered. It is possible though that there are different reasons behind that effect.

There was a single hardware setup (UM2 with 0.6 mm nozzle) considered in [25]. It was shown that printing speed has a dual effect on bonding strength. On one side, reducing layer printing time results in higher sublayer temperature, which has positive effect on sample strength. On the other hand, extrusion efficiency is reduced, which affects adversely the strength. Current study resulted in a different situation. First, printing with 0.4 mm nozzles did not result in significant sublayer temperature variance, thus, the positive effect of increasing printing speed is close to zero. Second, decrease in extrusion efficiency along with increased speed is registered only for Bowden-type extruders. Finally, the printing speed influences the strength through a badly formalized parameter of “printing accuracy” or “motion accuracy” in the system of the nozzle and already printed part of the sample. It was only the UM2 machine that had no issues with positioning accuracy with increased printing speed. All other machines had such or another issues, although they were different depending on the mechanics design (sample oscillations on a moving heated bed on PRUSA; nozzle colliding into the sample on delta printers, i.e. WASP and 3DQ). These have negative effect on sample strength.

More experiments with samples of different shape (different height to bed projection ratio) might bring better insight on the dependency of bonding strength on the printing speed will be more clear. That ratio defines the sample stability during printing on machines with moving bed or printing head causing oscillations along Z axis while printing flat XY layers (delta printers).

4.6 Layer thickness influence with respect to hardware setup

The distinctive feature of printers with Bowden-type extruder is the noticeable and sharp drop in unit strength along with layer thickness increase, correlated with reduced extrusion efficiency. This phenomenon is well illustrated by SEM scans of cross-sections of broken parts printed with different setups in [30]. The picture is less clear for printers with direct extruder (PRUSA) and with short Bowden tube (WASP). Samples printed on PRUSA machine at 25 mm/s linear motion speed exhibit slight strength increase when layer thickness is increased from 0.1 to 0.2mm, but given standard deviation calculated that increase is not statistically significant. On the other hand, for linear motion speed of 25 and 50 mm/s, increasing layer thickness from 0.25mm to 0.3mm results in a significant and perceptible reduction of sample strength. The similar decrement occurs when transitioning from 0.15 to 0.2 mm layer thickness at 75 mm/s speed. That could be explained by sample oscillations during printing process: at 0.2 mm layer thickness these oscillations have smaller effect, while sample with thin layers could be more sensitive.

The WASP printer exhibits the tendency towards strength drop along with layer thickness increase, but in some cases (layer thickness increase from 0.1 to 0.15mm at 25 mm/s and 75 mm/s) certain increase of strength is registered. Given repeatability of these results, that increase cannot be ignored. It should be noted that such increase was not registered at 50 mm/s printing speed.

It is possible that temperature conditions at layers boundary begin to play the most important role when increasing flow rate does not reduce extrusion efficiency. When the sample is printed with thicker layers, there are greater portions of hot polymer deposited, these contain proportionally larger amount of energy, and the latter is to larger extent transferred to the sublayer, melting it and creating better cohesion. The thermal imager used in current experiment set did not allow to analyze temperature conditions at each individual layer and the boundaries between them due to low resolution. At the same time, the accumulated effect of sample temperature increase registered is too low to explain possible strength growth along with layer thickness increase.

Anyway, even with extrusion efficiency of 1.0, the threads forming the sample will not be ideally rectangular (with sides equal to layer thickness and nozzle diameter respectively), but still retain the barrel shape, being squeezed between the nozzle and the sublayer. The morphology of layer boundary is in details explained in [25]. Thus, FFF printing process results inevitably in voids and cavities formation at the boundaries of individual threads, and the projection of these voids onto XY plane grows in area along with layer thickness increase. That effect is clearly registered for all layer thickness range considered for Bowden-type machines, the direct and short Bowden extruder ones exhibit it only when exceeding certain limit (0.2-0.25mm) of layer thickness.

More research is required for printers with direct extruders to establish connection between geometrical parameters of the FFF process and layer cohesion strength. It is possible that the effect of layer thickness will be more clear if there is more data for broader range of layer thicknesses and other nozzle diameters, as it was done for Bowden-type extruder in [25, 30].

5 Conclusions

Mechanical design and build quality of the specific 3D printer can both have quantitative and qualitative effect on printed samples strength w.r.t. geometrical and technological parameters of FFF process. The researchers should be careful when interpreting the results of any experiments: the

dependency discovered might only be applicable for the specific class of the FFF devices on which the experiments were run.

Among all hardware features of the printers considered in the current study, the most important one seems to be the extruder type. There are two kinds of them. The first one provides stable extrusion efficiency in the whole operational range of flow rates — these are direct extruders and Bowden extruders with a short tube. The second type of extruders features relatively long (~600 mm) flexible guiding tube. The latter one leads to decrease in performance (extrusion efficiency) with flow rate increased, which in turn results in significant strength reduction along with increased layer thickness or feed rate. It might be more correct to stipulate that distinguishing feature of a FFF 3D printer is the distance between the feeder and the nozzle rather than extruder type.

In spite of significant difference in hardware, all printers considered exhibit similar results when printing at relatively low printing speed (25 mm/s). That results can be approximated by the single regression model, including such parameters as layer thickness and extrusion efficiency.

Author Contributions: V.E.K. conceived and designed the experiments and wrote the paper; A.G.T. and O.D.U. performed the experiments.

Conflicts of Interest: The authors declare no conflict of interest.

References

1. Sculpteo's 4th annual report on 3D Printing and Digital Manufacturing. Available online https://www.sculpteo.com/en/get/report/state_of_3D_printing_2018/
2. Wohlers, T. Wohlers Report 2018: 3D Printing and Additive Manufacturing State of the Industry Annual Worldwide Progress Report; Wohlers Associates Inc.: Fort Collins, CO, USA, 2018.
3. Wohlers, T. Wohlers Report 2019: 3D Printing and Additive Manufacturing State of the Industry; Wohlers Associates Inc.: Fort Collins, CO, USA, 2019.
4. Sells, E.; Bailard, S.; Smith, Z.; Bowyer, A.; Olliver, V. RepRap: The Replicating Rapid Prototyper-Maximizing Customizability by Breeding the Means of Production. In Proceedings of the World Conference on Mass Customization and Personalization, Cambridge, MA, USA, 7–10 October 2007.
5. The RepRap project. Available online: https://reprap.org.
6. Jones, R.; Haufe, P.; Sells, E.; Iravani, P.; Olliver, V.; Palmer, C.; Bowyer, A. RepRap-the Replicating Rapid Prototyper. Robotica 2011, 29, 177–191.
7. Bowyer, A. 3D Printing and Humanity's First Imperfect Replicator. 3D Print. Addit. Manuf. 2014, 1, 4–5.
8. Crump, S. Apparatus and Method for Creating Three-Dimensional Objects. U.S. Patent 5121329, 30 October 1989.
9. Crump S. Fast, Precise, Safe Prototype with FDM. ASME PED 1991, 50, 53–60.
10. Crump S. The extrusion process of fused deposition modeling. In Proceedings of the 3rd International Conference on Rapid Prototyping, Dayton, OH, USA, 7–10 June 1992.
11. E. Fodran, M. Koch, U. Menon. Mechanical and dimensional characteristics of fused deposition modeling build styles. Solid Freeform Fabrication Proceedings (1996), pp. 419-442

12. M. Bertoldi, M. Yardimci, C. Pistor, S. Guceri, G. Sala. Mechanical characterization of parts processed via fused deposition. Proceedings of Solid Freeform Fabrication Symposium (1998), pp. 557-565
13. O. S. Es-Said, J. Foyos, R. Noorani, M. Mendelson, R. Marloth & B. A. Pregger (2000) Effect of Layer Orientation on Mechanical Properties of Rapid Prototyped Samples, Materials and Manufacturing Processes, 15:1, 107-122, DOI: 10.1080/10426910008912976
14. Rodríguez, J. F., Thomas, J. P., & Renaud, J. E. (2001). Mechanical behavior of acrylonitrile butadiene styrene (ABS) fused deposition materials. Experimental investigation. *Rapid Prototyping Journal*, *7*(3), 148-158.
15. Ahn, S. H., Montero, M., Odell, D., Roundy, S., & Wright, P. K. (2002). Anisotropic material properties of fused deposition modeling ABS. *Rapid prototyping journal*, *8*(4), 248-257.
16. Sun, Q., Rizvi, G. M., Bellehumeur, C. T., & Gu, P. (2008). Effect of processing conditions on the bonding quality of FDM polymer filaments. *Rapid Prototyping Journal*, *14*(2), 72-80.
17. Sood, A. K., Ohdar, R. K., & Mahapatra, S. S. (2010). Parametric appraisal of mechanical property of fused deposition modelling processed parts. *Materials & Design*, *31*(1), 287-295.
18. Sood, A. K., Ohdar, R. K., & Mahapatra, S. S. (2012). Experimental investigation and empirical modelling of FDM process for compressive strength improvement. *Journal of Advanced Research*, *3*(1), 81-90.
19. Durgun, I., & Ertan, R. (2014). Experimental investigation of FDM process for improvement of mechanical properties and production cost. *Rapid Prototyping Journal*, *20*(3), 228-235.
20. Ziemian, S., Okwara, M., & Ziemian, C. W. (2015). Tensile and fatigue behavior of layered acrylonitrile butadiene styrene. *Rapid Prototyping Journal*, *21*(3), 270-278.
21. Onwubolu, G. C., & Rayegani, F. (2014). Characterization and optimization of mechanical properties of ABS parts manufactured by the fused deposition modelling process. *International Journal of Manufacturing Engineering*, *2014*.
22. Torres, J., Cole, M., Owji, A., DeMastry, Z., & Gordon, A. P. (2016). An approach for mechanical property optimization of fused deposition modeling with polylactic acid via design of experiments. *Rapid Prototyping Journal*, *22*(2), 387-404.
23. Deng, X., Zeng, Z., Peng, B., Yan, S., & Ke, W. (2018). Mechanical properties optimization of poly-ether-ether-ketone via fused deposition modeling. *Materials*, *11*(2), 216.
24. Yang, T. C. (2018). Effect of extrusion temperature on the physico-mechanical properties of unidirectional wood fiber-reinforced polylactic acid composite (WFRPC) components using fused deposition modeling. *Polymers*, *10*(9), 976.
25. Kuznetsov, V. E., Solonin, A. N., Tavitov, A. G., Urzhumtsev, O. D., & Vakulik, A. H. (2018). Increasing of Strength of FDM (FFF) 3D Printed Parts by Influencing on Temperature-Related Parameters of the Process.
26. Rankouhi, B., Javadpour, S., Delfanian, F., & Letcher, T. (2016). Failure analysis and mechanical characterization of 3D printed ABS with respect to layer thickness and orientation. *Journal of Failure Analysis and Prevention*, *16*(3), 467-481.
27. Lanzotti, A., Grasso, M., Staiano, G., & Martorelli, M. (2015). The impact of process parameters on mechanical properties of parts fabricated in PLA with an open-source 3-D printer. *Rapid Prototyping Journal*, *21*(5), 604-617.
28. Torres, J., Cotelo, J., Karl, J., & Gordon, A. P. (2015). Mechanical property optimization of FDM PLA in shear with multiple objectives. *Jom*, *67*(5), 1183-1193.

29. Chacón, J. M., Caminero, M. Á., García-Plaza, E., & Núñez, P. J. (2017). Additive manufacturing of PLA structures using fused deposition modelling: Effect of process parameters on mechanical properties and their optimal selection. *Materials & Design*, *124*, 143-157.
30. Kuznetsov, V., Solonin, A., Urzhumtsev, O., Schilling, R., & Tavitov, A. (2018). Strength of PLA components fabricated with fused deposition technology using a desktop 3D printer as a function of geometrical parameters of the process. *Polymers*, *10*(3), 313.
31. Rodríguez-Panes, A., Claver, J., & Camacho, A. (2018). The Influence of Manufacturing Parameters on the Mechanical Behaviour of PLA and ABS Pieces Manufactured by FDM: A Comparative Analysis. *Materials*, *11*(8), 1333. MDPI AG. Retrieved from http://dx.doi.org/10.3390/ma11081333
32. Li, H., Wang, T., Sun, J., & Yu, Z. (2018). The effect of process parameters in fused deposition modelling on bonding degree and mechanical properties. *Rapid Prototyping Journal*, *24*(1), 80-92.
33. Tanikella, N. G., Wittbrodt, B., & Pearce, J. M. (2017). Tensile strength of commercial polymer materials for fused filament fabrication 3D printing. *Additive Manufacturing*, *15*, 40-47.
34. Cantrell, J. T., Rohde, S., Damiani, D., Gurnani, R., DiSandro, L., Anton, J., ... & Ifju, P. G. (2017). Experimental characterization of the mechanical properties of 3D-printed ABS and polycarbonate parts. *Rapid Prototyping Journal*, *23*(4), 811-824.
35. Fernandez-Vicente, M., Calle, W., Ferrandiz, S., & Conejero, A. (2016). Effect of infill parameters on tensile mechanical behavior in desktop 3D printing. *3D printing and additive manufacturing*, *3*(3), 183-192.
36. Alvarez, C., Kenny, L., Lagos, C., Rodrigo, F., & Aizpun, M. (2016). Investigating the influence of infill percentage on the mechanical properties of fused deposition modelled ABS parts. *Ingeniería e Investigación*, *36*(3), 110-116.
37. Mahmood, S., Qureshi, A. J., Goh, K. L., & Talamona, D. (2017). Tensile strength of partially filled FFF printed parts: experimental results. *Rapid Prototyping Journal*, *23*(1), 122-128.
38. Ebel, E., & Sinnemann, T. (2014). Fabrication of FDM 3D objects with ABS and PLA and determination of their mechanical properties. *RTejournal*, *2014*(1).
39. Lubombo, C., & Huneault, M. A. (2018). Effect of infill patterns on the mechanical performance of lightweight 3D-printed cellular PLA parts. *Materials Today Communications*, *17*, 214-228.
40. Kuznetsov, V.E.; Tavitov, A.G.; Urzhumtsev, O.D.; Mikhalin, M.V.; Solonin, A.N. (2019). Design and Fabrication of Strong Parts from Poly (Lactic Acid) with a Desktop 3D Printer: A Case with Interrupted Shell. *Polymers*, *11*(5), 760. doi:10.3390/polym11050760
41. ASTM D638-14, Standard Test Method for Tensile Properties of Plastics, ASTM International, West Conshohocken, PA, 2014, www.astm.org
42. ASTM D790-17, Standard Test Methods for Flexural Properties of Unreinforced and Reinforced Plastics and Electrical Insulating Materials, ASTM International, West Conshohocken, PA, 2017, www.astm.org
43. Popescu, D., Zapciu, A., Amza, C., Baciu, F., & Marinescu, R. (2018). FDM process parameters influence over the mechanical properties of polymer specimens: A review. *Polymer Testing*, *69*, 157-166.
44. https://github.com/daid/LegacyCura
45. https://www.flir.com/products/flir-tools/